Differentially heated flow from a rotating sphere

N. Leung[1], S. J. D. D'Alessio[2] & J. W. L. Wan[2]
[1]*Department of Computer Science, University of Toronto, Canada*
[2]*Faculty of Mathematics, University of Waterloo, Canada*

Abstract

We present results on the flow of a thin fluid layer over a rotating sphere having a surface temperature that varies with latitude. The fluid is taken to be viscous, incompressible and Newtonian while the flow is assumed to possess both azimuthal and equatorial symmetry. The governing Navier–Stokes and energy equations are formulated in terms of a stream function and vorticity. An approximate analytical solution for the steady-state flow has been derived and is compared with numerical solutions to the steady and unsteady governing equations. For small Rayleigh numbers these solutions are found to be in close agreement. However, as the Rayleigh number is increased noticeable differences occur. A numerical solution procedure is presented along with a procedure for obtaining an approximate analytical solution.
Keywords: Rayleigh–Bénard convection, rotation, heat transfer, shallow flow, analytical, numerical.

1 Introduction

The flow and heat transfer from a differentially heated rotating sphere are of interest in geophysical and meteorological applications such as weather prediction and climate modelling. These flows are intrinsically complicated because of the combination of differential heating, rotation and stratification of the atmosphere. Rather than solving an ambitiously difficult problem crudely, as done by General Circulation Models (GCMs), the aim here will be to tackle a much simpler problem and to solve it accurately. A recent related study is that of Lewis and Langford [1] which represents a numerical investigation into the stability of the steady-state flow.

WIT Transactions on Engineering Sciences, Vol 82, © 2014 WIT Press
www.witpress.com, ISSN 1743-3533 (on-line)
doi:10.2495/AFM140241

2 Governing equations

By treating the atmosphere as a thin fluid layer, a simple mathematical model governing the unsteady laminar convective flow of a viscous incompressible dry Boussinesq fluid from a solid rotating differentially heated sphere can be formulated. In the rotating reference frame the fluid is initially at rest and is set into motion by buoyancy as a result of a prescribed poleward decrease in surface temperature as well as a radial decrease in temperature as illustrated in figure 1. The poleward decrease in surface temperature mimics solar heating and is taken to be sinusoidal since this is consistent with the amount of solar radiation penetrating into the surface as it tilts away from the equator. In addition, the flow is assumed to possess both azimuthal and equatorial symmetry.

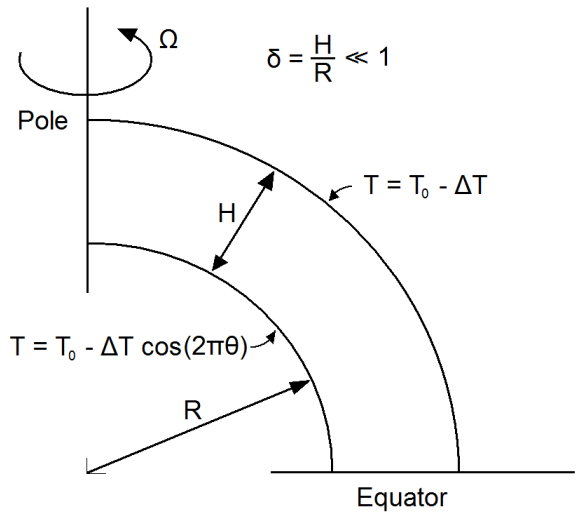

Figure 1: Flow set up.

Owing to the assumed symmetry, the governing unsteady Navier–Stokes and energy equations can be expressed in terms of a stream function (ψ) and vorticity (ω). The velocity components v_r, v_θ in the r, θ directions, respectively, are related to the stream function through the relations:

$$v_r = \frac{1}{r^2 \sin\theta}\frac{\partial \psi}{\partial \theta}\ ,\ v_\theta = -\frac{1}{r \sin\theta}\frac{\partial \psi}{\partial r}$$

In spherical coordinates (r, θ) and cast in dimensionless form the equations can be formulated as [2]:

$$\omega = -\delta D^2 \psi \tag{1}$$

$$\frac{\partial \omega}{\partial t} + \frac{\delta}{r^2 \sin\theta}\frac{\partial(\psi, \omega)}{\partial(\theta, r)} + \delta Pr Ra \sin\theta \frac{\partial T}{\partial \theta} + \frac{2\delta\omega}{r^2 \sin^2\theta}\left(\cos\theta \frac{\partial \psi}{\partial r} - \frac{\sin\theta}{r}\frac{\partial \psi}{\partial \theta}\right)$$

$$-\left(\frac{2\delta^2 W}{r^2\sin^2\theta}+\frac{2\delta^2}{Ro}\right)\left(\cos\theta\frac{\partial W}{\partial r}-\frac{\sin\theta}{r}\frac{\partial W}{\partial\theta}\right)=\delta^2 PrD^2\omega \tag{2}$$

$$\delta^2 PrD^2W-\frac{\partial W}{\partial t}=\frac{\delta}{r^2\sin\theta}\frac{\partial(\psi,W)}{\partial(\theta,r)}-\frac{2\delta}{Ro}\left(\cos\theta\frac{\partial\psi}{\partial r}-\frac{\sin\theta}{r}\frac{\partial\psi}{\partial\theta}\right) \tag{3}$$

$$\frac{\partial T}{\partial t}+\frac{\delta}{r^2\sin\theta}\frac{\partial(\psi,T)}{\partial(\theta,r)}=\delta^2\nabla^2 T \tag{4}$$

In the above t denotes time, r is the radial coordinate, and θ is the angle with the polar axis. The flow variable W denotes the scaled zonal velocity while T is the scaled temperature. The dimensionless parameters appearing in the above equations include the Rayleigh number (Ra), the Rossby number (Ro), the Prandtl number (Pr) and the shallowness parameter (δ) which are defined as follows:

$$Ra=\frac{\alpha g H^3\Delta T}{\nu\kappa}\ ,\ Ro=\frac{\kappa}{H\Omega R}\ ,\ Pr=\frac{\nu}{\kappa}\ ,\ \delta=\frac{H}{R}$$

Here, the fluid properties ν,κ and α represent the kinematic viscosity, thermal diffusivity and thermal expansion coefficient, respectively, whereas g is the acceleration due to gravity, R is the radius of the sphere, H is the thickness of the fluid layer, ΔT is the maximum temperature difference between the surface and the top of the fluid layer, and Ω is the rotation rate about the polar axis. In deriving the vorticity transport equation (2) we have made the Boussinesq approximation whereby the fluid density (ρ) varies linearly with temperature according to:

$$\rho=\rho_r[1-\alpha(T-T_r)]$$

where ρ_r represents the reference density corresponding to temperature T_r. The time and length are scaled as follows:

$$\tilde{t}\rightarrow\frac{H^2}{\kappa}t\ ,\ \tilde{r}\rightarrow Rr$$

whereas the adopted scaling for the flow variables is given by:

$$(\tilde{\psi},\tilde{\omega},\tilde{W},\tilde{T})\rightarrow(\frac{\kappa R^2}{H}\psi,\frac{\kappa R}{H^2}\omega,\frac{\kappa R}{H}W,T_a+(\Delta T)T)$$

In the above, the tilde denotes a dimensional quantity and T_a the constant ambient temperature. Lastly, the differential operators D^2,∇^2 and $\partial(A,B)/\partial(x,y)$ are

defined as follows:

$$D^2 = \frac{\partial^2}{\partial r^2} + \frac{1}{r^2}\frac{\partial^2}{\partial \theta^2} - \frac{\cot\theta}{r^2}\frac{\partial}{\partial \theta}$$

$$\nabla^2 = \frac{\partial^2}{\partial r^2} + \frac{2}{r}\frac{\partial}{\partial r} + \frac{1}{r^2}\frac{\partial^2}{\partial \theta^2} + \frac{\cot\theta}{r^2}\frac{\partial}{\partial \theta}$$

$$\frac{\partial(A,B)}{\partial(x,y)} = \frac{\partial A}{\partial x}\frac{\partial B}{\partial y} - \frac{\partial A}{\partial y}\frac{\partial B}{\partial x}$$

Equations (1)–(4) are to be solved in the region:

$$0 \le \theta \le \frac{\pi}{2}\,,\ 1 \le r \le 1+\delta$$

subject to the no-slip boundary conditions given by:

$$\psi = \frac{\partial \psi}{\partial r} = W = 0 \ \text{ on } \ r = 1 \ \text{ and } \ r = 1+\delta$$

The assumed symmetry requires that we impose the following conditions at the pole and equator:

$$\psi = \omega = W = 0 \ \text{ along } \ \theta = 0 \ \text{ and } \ \psi = \omega = \frac{\partial W}{\partial \theta} = 0 \ \text{ along } \ \theta = \frac{\pi}{2}$$

We observe that the stream function is overspecified while the vorticity is underspecified. Later we will explain how the extra conditions for the stream function can be used to furnish the missing conditions for the vorticity. The temperature, on the other hand, satisfies:

$$T = 1 - \gamma\cos^2\theta \ \text{ on } \ r = 1 \ \text{ and } \ T = 0 \ \text{ on } \ r = 1+\delta$$

where the parameter γ represents the ratio of the maximum difference in surface temperature and the maximum difference in temperature between the surface and the top of the fluid layer. The dimensionless temperature has been scaled so that the maximum difference in temperature between the surface and the top of the fluid layer is unity, and the constant temperature at the top of the fluid layer is zero. At the pole ($\theta = 0$) and the equator ($\theta = \pi/2$) we apply the zero heat-flux/Neumann condition:

$$\frac{\partial T}{\partial \theta} = 0 \ \text{ along } \ \theta = 0 \ \text{ and } \ \theta = \frac{\pi}{2}$$

As previously mentioned, the fluid is initially taken to be at rest having a temperature distribution given by the approximate analytical solution derived in the next section.

3 Analytical and numerical methods

For analytical and numerical purposes we propose a change of coordinates and introduce (z, μ) where $r = 1 + \delta z$ and $\mu = \cos\theta$. This has the advantage of mapping the computational domain to the unit square: $0 \leq z, \mu \leq 1$. On the unit square, the transformed equations read:

$$\delta\omega = -\hat{D}^2\psi \tag{5}$$

$$\begin{aligned}&\frac{\partial\omega}{\partial t} + \frac{1}{(1+\delta z)^2}\frac{\partial(\psi,\omega)}{\partial(z,\mu)} + \frac{2\omega}{(1-\mu^2)(1+\delta z)^2}\left[\mu\frac{\partial\psi}{\partial z} + \frac{\delta(1-\mu^2)}{(1+\delta z)}\frac{\partial\psi}{\partial\mu}\right]\\ &- \frac{2\delta W}{(1-\mu^2)(1+\delta z)^2}\left[\mu\frac{\partial W}{\partial z} + \frac{\delta(1-\mu^2)}{(1+\delta z)}\frac{\partial W}{\partial\mu}\right]\\ &- \frac{2\delta}{R_0}\left[\mu\frac{\partial W}{\partial z} + \frac{\delta(1-\mu^2)}{(1+\delta z)}\frac{\partial W}{\partial\mu}\right] = \delta PrRa(1-\mu^2)\frac{\partial T}{\partial\mu} + Pr\hat{D}^2\omega\end{aligned} \tag{6}$$

$$\frac{\partial T}{\partial t} + \frac{1}{(1+\delta z)^2}\frac{\partial(\psi,T)}{\partial(z,\mu)} = \hat{\nabla}^2 T \tag{7}$$

$$Pr\hat{D}^2 W - \frac{\partial W}{\partial t} = \frac{1}{(1+\delta z)^2}\frac{\partial(\psi,W)}{\partial(z,\mu)} - \frac{2}{R_0}\left[\mu\frac{\partial\psi}{\partial z} + \frac{\delta(1-\mu^2)}{(1+\delta z)}\frac{\partial\psi}{\partial\mu}\right] \tag{8}$$

The transformed differential operators become:

$$\hat{D}^2 = \frac{\partial^2}{\partial z^2} + \frac{\delta^2(1-\mu^2)}{(1+\delta z)^2}\frac{\partial^2}{\partial\mu^2}$$

$$\hat{\nabla}^2 = \frac{\partial^2}{\partial z^2} + \frac{2\delta}{(1+\delta z)}\frac{\partial}{\partial z} - \frac{2\mu\delta^2}{(1+\delta z)^2}\frac{\partial}{\partial\mu} + \frac{\delta^2(1-\mu^2)}{(1+\delta z)^2}\frac{\partial^2}{\partial\mu^2}$$

We point out that the zero heat-flux/Neumann condition becomes:

$$\frac{\partial T}{\partial\theta} = -\sqrt{1-\mu^2}\frac{\partial T}{\partial\mu} = 0$$

This is problematic at the pole since the factor $\sqrt{1-\mu^2} = 0$ when $\mu = 1$. To overcome this difficulty we replace this condition with

$$T = (1-\gamma)(1-z)(1-\delta z) + \delta^2 T_2(z, \mu = 1)$$

at the pole, where T_2 is to be defined. As we will shortly see, this condition is consistent with the approximate analytical solution which is derived below.

For small δ approximate analytical solutions can be constructed by expanding the flow variables in the following series:

$$\psi = \psi_0 + \delta\psi_1 + \delta^2\psi_2 + \cdots$$

$$\omega = \omega_0 + \delta\omega_1 + \delta^2\omega_2 + \cdots$$

$$W = W_0 + \delta W_1 + \delta^2 W_2 + \cdots$$

$$T = T_0 + \delta T_1 + \delta^2 T_2 + \cdots$$

Using the above expansions it is a straight-forward exercise to show that $\psi_0 = \psi_1 = \omega_0 = W_0 = W_1 = 0$ as well as to determine the non-zero terms $\psi_2, \omega_1, \omega_2, W_2, T_0, T_1$ and T_2. For the steady-state equations the approximate solutions, correct to second order in δ, are given by:

$$\psi_s(z,\mu) \approx -2\gamma\delta^2 Ra\mu(1-\mu^2)F_1(z)$$

$$\omega_s(z,\mu) \approx 2\gamma\delta Ra\mu(1-\mu^2)[F_1{}''(z) + \delta F_2(z)]$$

$$W_s(z,\mu) \approx \frac{4\gamma\delta^2 Ra}{PrR_0}\mu^2(1-\mu^2)F_3(z)$$

$$T_s(z,\mu) \approx (1-\gamma\mu^2)(1-z)(1-\delta z) + \delta^2 T_2(z,\mu)$$

where

$$F_1(z) = \frac{z^4}{24} - \frac{z^5}{120} - \frac{7z^3}{120} + \frac{z^2}{40}$$

$$F_2(z) = \frac{z^4}{12} - \frac{z^3}{6} + \frac{z}{12} - \frac{1}{60}$$

$$F_3(z) = \frac{z^5}{120} - \frac{z^6}{720} - \frac{7z^4}{480} + \frac{z^3}{120} - \frac{z}{1440}$$

$$T_2(z,\mu) = \gamma(1-3\mu^2)z^2\left(1-\frac{z}{3}\right) + (1-\gamma\mu^2)z^2\left(1-\frac{z^2}{3}\right)$$

$$+\gamma^2 Ra\mu^2(1-\mu^2)z^3F_4(z) - \gamma Ra(1-3\mu^2)(1-\gamma\mu^2)z^4F_5(z) + Kz$$

with

$$F_4(z) = \frac{z^4}{252} - \frac{z^3}{36} + \frac{41z^2}{600} - \frac{3z}{40} + \frac{1}{30}$$

$$F_5(z) = \frac{z^2}{360} - \frac{z^3}{2520} - \frac{7z}{1200} + \frac{1}{240}$$

$$K = -\frac{2}{3}(1-\gamma\mu^2) - \frac{2}{3}\gamma(1-3\mu^2) - \gamma^2 Ra\frac{\mu^2(1-\mu^2)}{350} + \gamma Ra\frac{(1-3\mu^2)(1-\gamma\mu^2)}{1400}$$

and the prime denotes differentiation with respect to z. These approximate analytical solutions will soon be used to validate the steady-state numerical solutions as well as the limiting unsteady numerical solutions for large t.

Equations (5)–(8) are solved by a finite difference method where the spatial derivatives are discretized by central differences and the time derivative by implicit time stepping [3]. Since we are working on a unit square, we take the grid spacing to be the same in both the z and μ directions. The corresponding steady-state equations are solved using a similar approach. The finite difference discretization for the steady and unsteady equations results in a system of coupled discrete nonlinear equations. Let $(\psi^n, \omega^n, T^n, W^n)$ denote the numerical solutions at time t_n with the initial condition at $t = t_0$ represented by $(\psi^0, \omega^0, T^0, W^0)$. At each time step, the solutions at time t_{n+1}, namely $(\psi^{n+1}, \omega^{n+1}, T^{n+1}, W^{n+1})$, are computed by solving the discrete nonlinear system using fixed point iteration described below.

Let $(\psi_k^{n+1}, \omega_k^{n+1}, T_k^{n+1}, W_k^{n+1})$ be an approximate solution after k fixed point iterations of $(\psi^{n+1}, \omega^{n+1}, T^{n+1}, W^{n+1})$. We take the initial guess to be

$$(\psi_0^{n+1}, \omega_0^{n+1}, T_0^{n+1}, W_0^{n+1}) = (\psi^n, \omega^n, T^n, W^n)$$

which corresponds to the solution at the previous time step. The iteration procedure starts by solving equation (7) for T_{k+1}^{n+1} using the known value of ψ_k^{n+1}. Similarly, we solve equation (8) to obtain W_{k+1}^{n+1} using the current state ψ_k^{n+1}. The boundary conditions for these two variables are handled using a standard approach, with the Neumann conditions being discretized along the corresponding boundaries.

The determination of ω_{k+1}^{n+1} and ψ_{k+1}^{n+1}, however, requires more care. We note that there are six boundary conditions for ψ and two boundary conditions for ω. The stream function ψ has two boundary conditions at both $z = 0$ and $z = 1$, while ω has none. The lack of boundary conditions at $z = 0$ and $z = 1$ leads to an incomplete system for ω, when (5) is discretized. Various methods have been advanced to deal with this. One involves the use of so-called integral conditions which are explained in [4].

Our strategy for solving (5) and (6) is as follows. In the $(k + 1)$-th iteration, we view (5) and (6) as a joint system, and we seek to simultaneously determine ω_{k+1}^{n+1} and ψ_{k+1}^{n+1}. Let m be the number of *interior* grid points in the z or μ direction. For ψ we need m^2 equations because $\psi = 0$ on the boundary. For ω, however, we need $m^2 + 2m$ equations because the values of ω are unknown along $z = 0$ and $z = 1$. We have m^2 equations from (6). The remaining $2m$ equations are inferred from the extra boundary conditions for ψ, as follows.

We extend the grid and assume that (5) holds at $z = 0$ and $z = 1$. Adopting the notation $f_{i,j} \equiv f(z_i, \mu_j)$ where $z_i = ih, \mu_j = jk$ with h, k denoting the uniform grid spacing in the z, μ directions, respectively, and discretizing (5) using central differences leads to:

$$\delta\omega_{i,j} = -\frac{(\psi_{i+1,j} - 2\psi_{i,j} + \psi_{i-1,j})}{h^2} - \frac{\delta^2(1-\mu_j^2)}{(1+\delta z_i)^2}\frac{(\psi_{i,j+1} - 2\psi_{i,j} + \psi_{i,j-1})}{k^2}$$

where in our case $h = k$. Using the condition $\psi_{i,j} = \psi_{i,j\pm1} = 0$ along the boundaries $z = 0$ and $z = 1$, the above simplifies to:

$$\delta\omega_{i,j} = -\frac{(\psi_{i+1,j} + \psi_{i-1,j})}{h^2}.$$

Along the line $z = 0$ the unknown $\psi_{i-1,j}$ lies outside the domain while along $z = 1$ the unknown $\psi_{i+1,j}$ lies outside the domain. These quantities can be eliminated by making use of the condition $\partial\psi/\partial z = 0$ along $z = 0$ and $z = 1$ which yields $\psi_{i-1,j} = \psi_{i+1,j}$ along these lines. Thus, the surface vorticity (i.e. $z = 0$) is given by the second-order finite-difference expression

$$\omega_{i,j} = -\frac{2\psi_{i+1,j}}{\delta h^2}$$

while on $z = 1$ the corresponding expression is

$$\omega_{i,j} = -\frac{2\psi_{i-1,j}}{\delta h^2}.$$

These expressions determine the remaining $2m$ equations. When put together, we have $2m^2+2m$ equations for the same number of unknowns. This approach results in a system that is about four times bigger than what would have been obtained if (ψ, ω) were decoupled. However, the system is still sparse, and can be solved rapidly using efficient algorithms.

This completes one iteration of the fixed point method. Iterations are repeated until convergence is reached using the stopping criterion:

$$||(\psi^{n+1}_{k^*+1}, \omega^{n+1}_{k^*+1}, T^{n+1}_{k^*+1}, W^{n+1}_{k^*+1}) - (\psi^{n+1}_{k^*}, \omega^{n+1}_{k^*}, T^{n+1}_{k^*}, W^{n+1}_{k^*})||_\infty < 10^{-6}.$$

From our experience, for Ra below a critical value, it usually takes only a few iterations ($k^* < 10$) to reach this criterion. When convergence is reached, we assign the converged values to be the solutions at the next time step, that is,

$$(\psi^{n+1}, \omega^{n+1}, T^{n+1}, W^{n+1}) = (\psi^{n+1}_{k^*+1}, \omega^{n+1}_{k^*+1}, T^{n+1}_{k^*+1}, W^{n+1}_{k^*+1}) \, .$$

4 Results

Numerical solutions to the steady and unsteady equations have been obtained. In our computations we have set $\gamma = 0.5$, $Ro = 1$, $\delta = 0.1$, $Pr = 0.7$ while the parameter Ra was varied. The adopted computational grid size was 80×80 implying a uniform grid spacing of $1/80$. For the unsteady computations the uniform time step $\Delta T = 0.01$ was used with initial conditions $W = \psi = \omega = 0$ and $T = T_s(z, \mu)$.

Shown in figure 2 is a contour plot of the steady-state stream function for $Ra = 1000$. The plot resembles a Hadley-type meridional cell whereby warmer air rises at the equator and sinks at the pole. Next we present the steady-state surface vorticity for $Ra = 2000$ shown in figure 3. Also plotted is the approximate

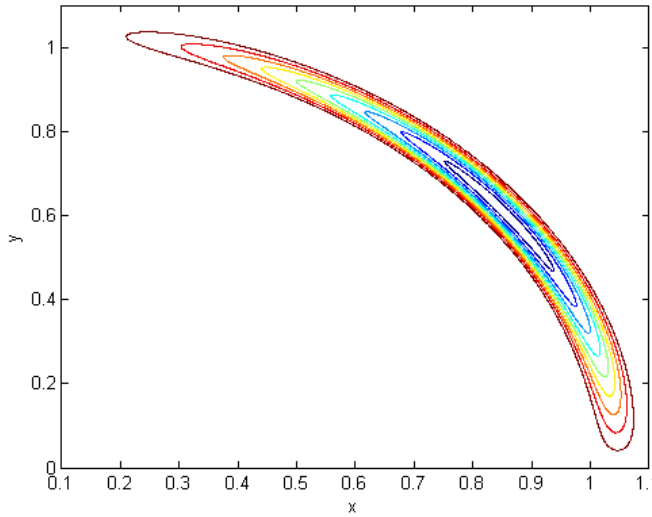

Figure 2: Streamline circulation pattern.

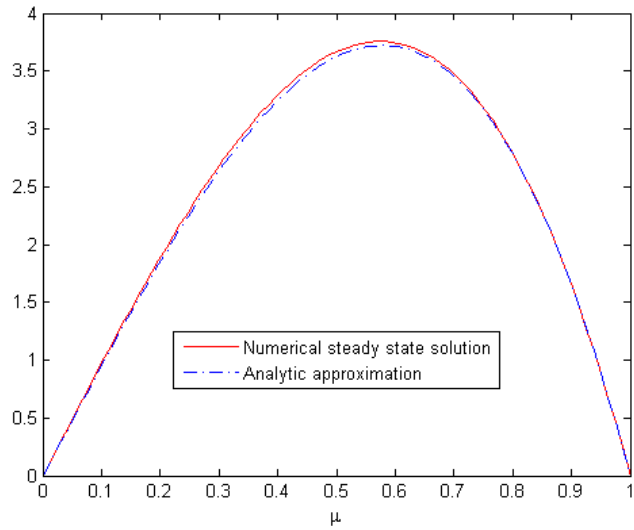

Figure 3: Surface vorticity comparison.

analytical solution; the two solutions are clearly in close agreement. Overall, good agreement between the steady-state and approximate analytical solutions was found in all the flow variables for Rayleigh numbers up to about 2000. In addition,

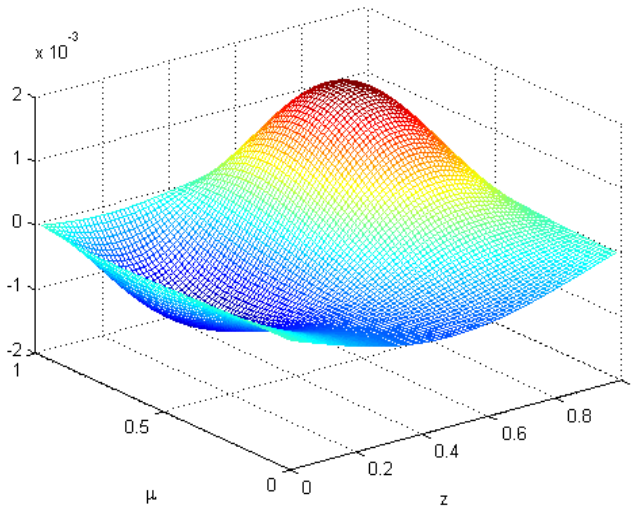

Figure 4: The zonal velocity distribution.

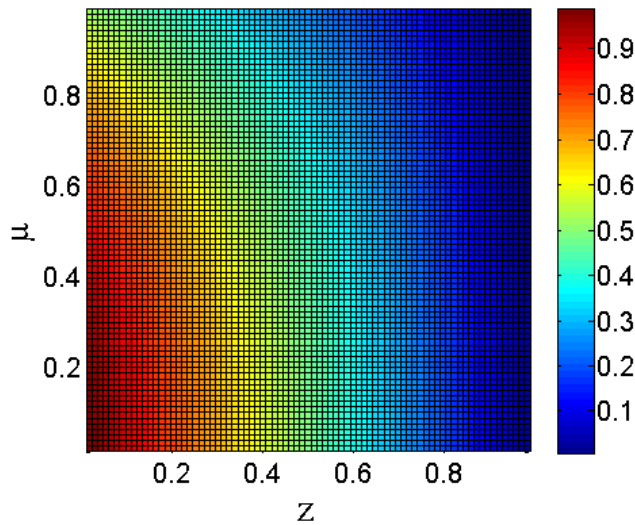

Figure 5: The temperature distribution.

the unsteady solutions converged to the steady-state solutions. A mesh plot of the steady-state zonal velocity is illustrated in figure 4 for $Ra = 2000$ and reveals a prominent peak. Based on the approximate analytical solution this peak is located

at $\mu = 1/\sqrt{2}$ (or $\theta = 45°$) at $z \approx 0.74$ and corresponds to a strong westerly flow which can be interpreted as the jet stream. Lastly, plotted in figure 5 is the steady-state temperature distribution for $Ra = 2000$.

As the Rayleigh number was increased beyond 2000 we encountered difficulties in reaching convergence in the steady-state solution. Further, the unsteady solution began to show noticeable departures from the steady-state solution. The formation of a small second cell near the pole started to appear in the unsteady solution which is likely the result of an instability.

This situation bears a close resemblance to the classical Rayleigh–Bénard convection problem [5, 6] which is well known to succumb to thermal instability.

5 Conclusions

Discussed in this work was an analytical and numerical investigation of the flow of a thin fluid layer over a rotating sphere. Our results revealed that for Rayleigh numbers up to about 2000 good agreement exists between the analytical and numerical solutions. However, as the Rayleigh number is increased the flow becomes unstable causing noticeable differences between the steady and unsteady numerical solutions. Future work will involve theoretically predicting the onset of instability. Additional results and plots will be discussed during the presentation.

Acknowledgements

Financial support for this research was provided by the Natural Sciences and Engineering Research Council of Canada and the Faculty of Mathematics at the University of Waterloo.

References

[1] Lewis, G.M. & Langford, W.F., Hysteresis in a rotating differentially heated spherical shell of Boussinesq fluid, *SIAM J. Appl. Dyn. Sys.*, **7**, pp. 1421–1444, 2008.
[2] Goldstein, S. (editor), *Modern Developments in Fluid Dynamics*, Clarendon Press, Oxford, UK (pp. 115), 1938.
[3] Leveque, R.J., *Finite Difference Methods for Ordinary and Partial Differential Equations: Steady-State and Time-dependent Problems*, Society for Industrial and Applied Mathematics, Philadelphia, USA, 2007.
[4] Dennis, S.C.R. & Quartapelle, L., Some uses of Greens theorem in solving the Navier–Stokes equations, *Int. J. Numer. Meth. Fluids*, **9**, pp. 871–890, 1989.
[5] Bénard, H., Les tourbillons cellulaires dans une mappe liquide, *Rev. Gen. Sci. Pures Appl.*, **11**, pp. 1261–1271, 1900.
[6] Drazin, P.G. & Reid, W.H., *Hydrodynamic Stability*, Cambridge University Press (second edition), Cambridge, UK, 2004.